D. B. Bogy
F. E. Talke

Experimental and Theoretical Study of Wave Propagation Phenomena in Drop-on-Demand Ink Jet Devices

This paper presents experimental observations and a theoretical analysis of the operation of drop-on-demand piezoelectric ink jet devices. By studying experimentally the dependence of several operating characteristics on the length of the cavity in the nozzle of an ink jet device, we have gained insight into the physical phenomena underlying the operation of such a device. It is concluded that drop-on-demand ink jet phenomena are related to the propagation and reflection of acoustic waves within the ink jet cavity. A simple analysis is carried out on the basis of linear acoustics which is in good agreement with the experimental observations.

Introduction

Published investigations of drop-on-demand ink jet technology have generally included the assumption that the fluid (ink) in the cavity of the ink jet nozzle is incompressible. Beasley [1] used quasi-steady continuity and incompressible momentum concepts to simulate the drop-ejection process in a fluid-filled tube surrounded by a short piezoelectric transducer. Using the notion of effective inertia and viscous lengths, he studied the different phases of the drop-formation process. Kyser et al, [2] modeled the cavity containing the ink by using a discrete parameter description with effective masses, springs, and equivalent damping coefficients.

A compressible analysis may be necessary for explaining several of the phenomena that have been observed experimentally. These phenomena appear to be related to the propagation and reflection of acoustic waves in the cavity; experimental results show that there exists a delay time between the application of a voltage signal and the first motion of the meniscus. Furthermore, propagating disturbances appear at the nozzle while the drop forms. Both of these phenomena depend on the length of the fluid-filled cavity, and, thus, indicate that drop-on-demand ink jet behavior may require the use of compressible equations for a correct description.

In this paper we present experimental results for the low-frequency drop-on-demand operation range, and we study the dependence of the operation characteristics on the length of the fluid cavity and the speed of acoustic wave propagation in the fluid. Linear acoustics is used to describe theoretically the wave propagation phenomena causing drop ejection. We consider the history of transient waves initiated by the motion of the piezoelectric transducer. Very good agreement is found to exist between predictions from our model and experimentally observed low-frequency characteristics of the drop-on-demand process, such as optimum voltage pulse width, delay time between pulse rise and meniscus motion, and period of meniscus oscillation.

Experimental setup and preliminary observations

The nozzle assembly used in the experimental investigations is shown schematically in **Figure 1.** It consists of a commercially available cylindrical piezoelectric tube (PZT-5H) which surrounds a glass capillary insert. The capillary insert and the PZT tube are of equal length and are bonded together. The tube assembly is supported on both ends by flexible washers and is coaxially aligned with channels of equal diameter. The two channels and the PZT tube assembly form the cavity of length l, as shown in Fig. 1. The inner and outer cylindrical surfaces of the PZT tube are nickel-plated to provide electrodes across which voltage pulses are applied. The front end of the cavity is terminated with a 0.125-mm-thick silicon plate, which contains a hole with an aperture dimension typically of 50 μm. The back end of the cavity is connected to a supply tube of larger diameter.

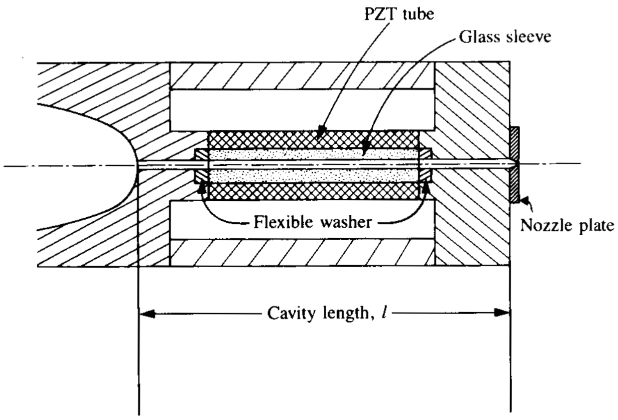

Figure 1 Schematic of ink jet nozzle assembly.

When a voltage pulse is applied across the inner and outer electrodes, a radial displacement of the tube is initiated. Depending on the polarization direction of the PZT, the inner radius can increase or decrease with a voltage increase. In general, a voltage pulse with a rise time of less than 3 μs was found to be sufficient for good drop ejection, but other pulse shape factors such as pulse width and voltage amplitude also affected the operation of the nozzle assembly. In order to keep the number of experimental parameters at a minimum in this investigation, we have used only rectangular voltage pulses. A study of the effect of pulse shapes on the drop-formation process can be found in [3]. In order to observe the drop-formation process after the voltage pulse is applied, use is made of a light-emitting diode which is strobed at the frequency of drop ejection. This freezes the drop and allows viewing on a TV monitor after suitable magnification.

From preliminary observations, we found that the drop-formation process and the frequency response of the nozzle assembly depend strongly on physical design parameters and fluid properties. In particular, we observed that the voltage pulse amplitude needed to eject a drop is lessened if the length of the PZT tube is increased. Furthermore, we observed that meniscus disturbances occur at the nozzle exit with a period that depends on the cavity length. These disturbances cause velocity variations of the ejected drops with frequency, and this in turn causes drop misregistration and print quality degradation in the case of asynchronous printing. In order to better understand the physical parameters that cause these phenomena and to gain insight into the optimization of the design of drop-on-demand multi-nozzle heads, a detailed study of single-nozzle assemblies with tubes of different lengths was undertaken.

Experimental observations

In Figure 2 we show the drop-formation process at 4-μs intervals for different cavity lengths. The nozzle was a silicon

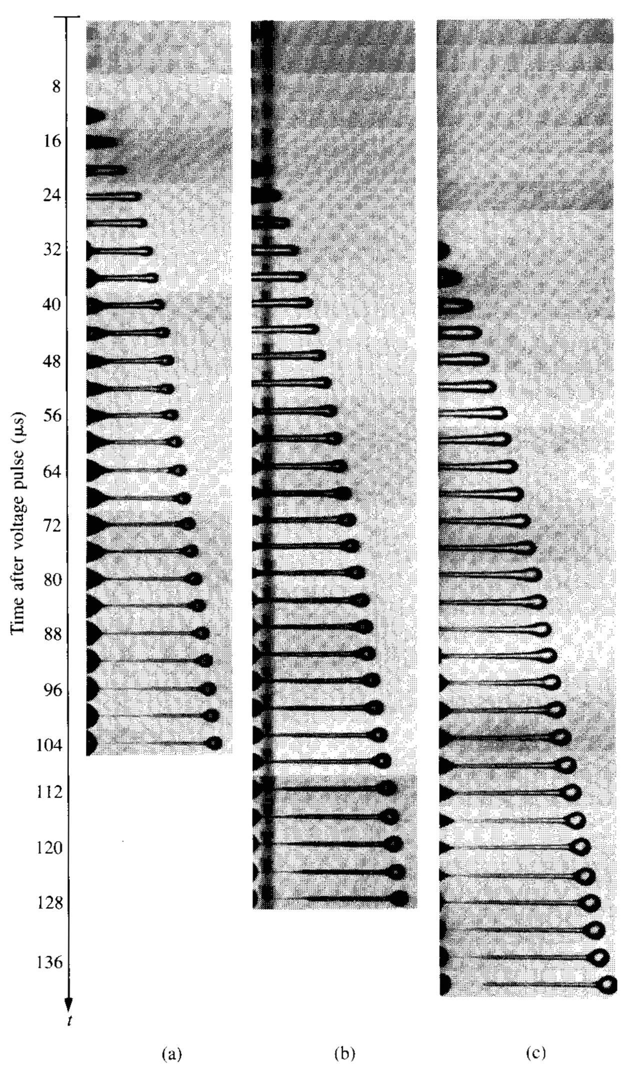

Figure 2 Drop-formation process at 4-μs intervals for cavity lengths of 12.3 mm (a), 18.7 mm (b), and 33.9 mm (c).

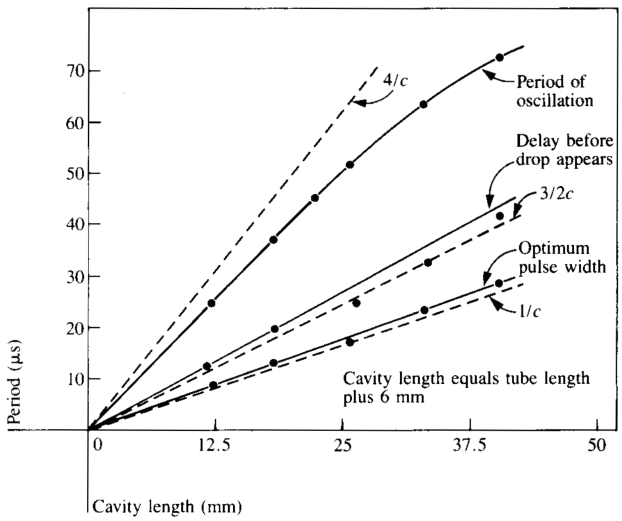

Figure 3 Period of oscillation, delay before appearance of drop, and optimum pulse width as a function of cavity length. Straight lines (dashed) having slopes of $4/c$, $3/2c$, and $1/c$ are also shown.

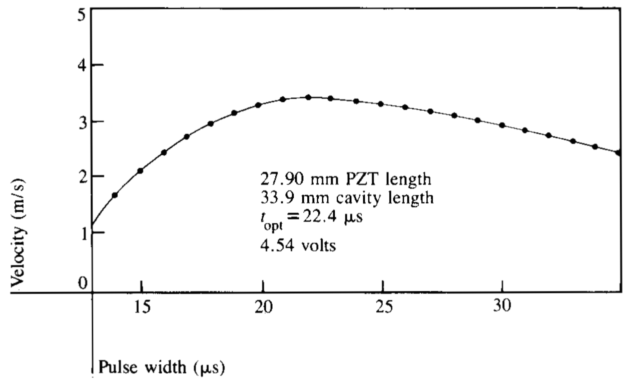

Figure 4 Drop velocity as a function of pulse width.

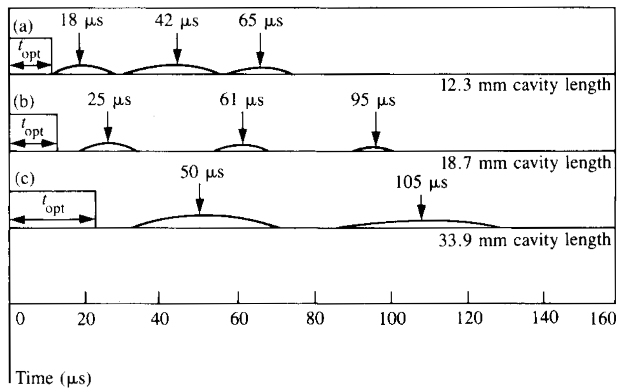

Figure 6 Meniscus protrusion from nozzle as a function of time after initial voltage rise.

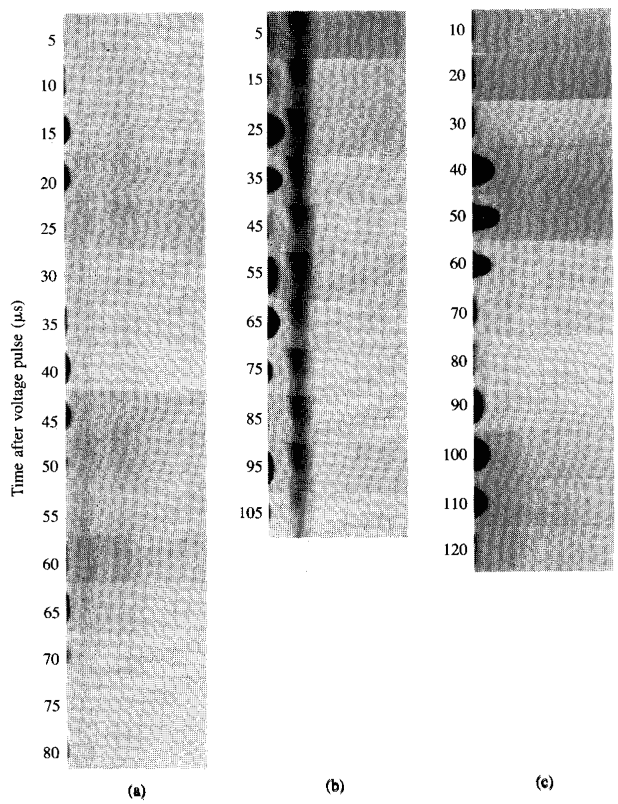

Figure 5 Time-dependent motion of the meniscus at 5- or 10-μs intervals. The sequences shown are for cavity lengths of 12.3 mm (a), 18.7 mm (b), and 33.9 mm (c).

nozzle of 50-μm aperture and the working fluid was ethylene glycol. From a close examination of the drop-formation sequences in Fig. 2, we can make the following observations. First, we note that a time delay t_d occurs between the initial voltage rise and the appearance of an outward moving meniscus from the orifice. The delays are about 12 μs, 20 μs, and 32 μs, respectively, for the different cavity lengths. As can be seen from the data in **Figure 3,** the time delay was found to be a linear function of the cavity length. That delay is apparently associated with the propagation inside the cavity of acoustic waves which interact with the meniscus at the nozzle to eject a drop. Its dependence on cavity length is characterized by a slope slightly more than $3/2c$, where c is the speed of acoustic waves in the fluid (1658 m/s for ethylene glycol at room temperature). Secondly, we observe that meniscus distortions occur during the drop-formation process at the base of the drop approximately $4l/c$ after the initial voltage rise and while the drop is still attached to the nozzle. In Fig. 2 these disturbances can first be observed at times of 32, 56, and 92 μs after the initial pulse rise for the three cavity lengths.

It should be pointed out that in all of the experiments we adjusted the voltage amplitude so that the ejected drops had a velocity of 3.5 m/s after separation. Before doing so, however, we optimized the pulse width by holding the voltage amplitude fixed and varying the pulse width until the maximum ejected-drop velocity was obtained. The pulse width was then held at this optimum value and its amplitude was adjusted to give the desired drop velocity. **Figure 4** shows the drop velocity at a pulse amplitude of 4.54 volts versus pulse width for a cavity length of 33.9 mm; the optimum pulse width, t_{opt}, was 8.2 μs. The lower curve in Fig. 3 shows the dependence of the experimentally determined values of t_{opt} on the length of the cavity. This latter dependence is seen to be approximately linear with a slope slightly more than $1/c$.

The observations that 1) an optimum pulse width exists which is a linear function of the cavity length; 2) there is a time delay of the meniscus motion that depends linearly on the cavity length; and 3) the meniscus distortion is related to the cavity length strongly suggest some correlation with acoustic waves which are generated by the contraction and expansion of the piezoelectric tube.

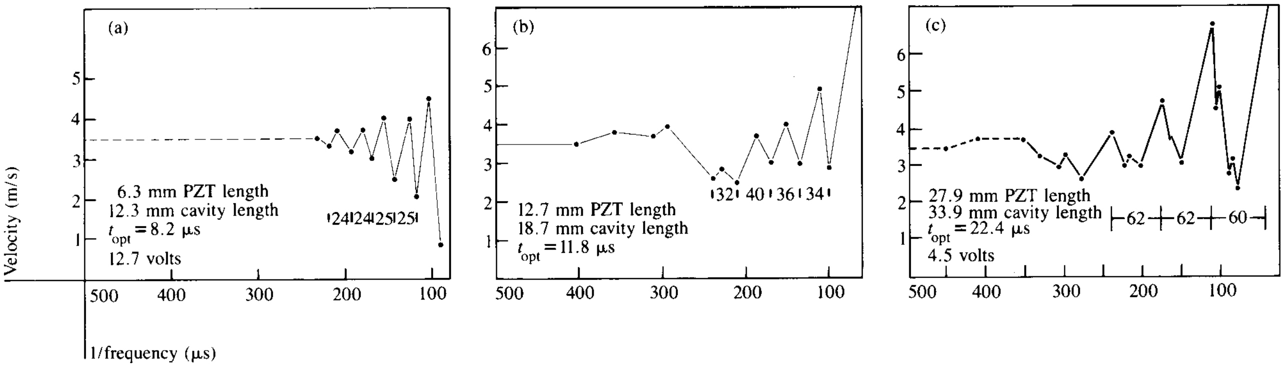

Figure 7 Synchronous drop velocity versus 1/frequency for cavity lengths of 12.3 mm (a), 18.7 mm (b), and 33.9 mm (c).

In order to examine the effects of acoustic pressure waves and to study their interaction with the meniscus, we investigated the motion of the meniscus after applying a low-amplitude voltage pulse to the PZT tube, i.e., a voltage pulse which was not strong enough to eject a drop from the nozzle. **Figure 5** shows the appearance of the meniscus at different times after the application of the pulse—for cavities of lengths 12.3 mm, 18.7 mm, and 33.9 mm, in time increments of 5 μs, 10 μs, and 10 μs, respectively. From Fig. 5 we have obtained **Figure 6,** which shows a graph of meniscus protrusion as a function of time after the initial voltage rise. Also shown are the optimum pulse widths, t_{opt}, in each case. As when a drop is ejected from the nozzle, a time delay occurs before the meniscus protrudes from the plane of the nozzle.

Finally, we measured the drop velocity as a function of synchronous drop-ejection frequency. **Figure 7** shows synchronous drop velocity versus 1/frequency for cavity lengths of 12.3 mm, 18.7 mm, and 33.9 mm, respectively. In each case we see that at low frequencies the velocity curves are relatively flat. Under those conditions, a long time has elapsed between adjacent pulses and the pressure from one pulse has decayed prior to the application of the subsequent pulse. At higher frequencies there are subharmonic resonance and antiresonance characteristics in the velocity-frequency curves, indicating that a multiply reflecting pressure pulse may be beneficial or detrimental, depending on the synchronization. The period between adjacent peaks is again a function of cavity length and is seen in Fig. 3 to be approximately $4l/c$.

Theoretical description

The experimental results presented in the preceding section indicate that the reinforcement, with proper time phase, of propagating pressure pulses may be the dominant mechanism in the operation of drop-on-demand devices at frequencies in the 1–15-kHz range. A complete theoretical understanding of this type phenomenon would need to be based on propagating wave solutions of the appropriate compressible fluid dynamic equations. Also, it would be necessary to obtain the proper reflection coefficients at the ends of the cavity.

For a first approximation, we consider linear acoustics and examine one-dimensional wave propagation in the fluid contained in the cavity shown in Fig. 1. We assume that the cavity is closed at the nozzle plate end and open at the other (supply) end. We also assume that the contraction or expansion of the inner radius of the PZT tube, as a result of the applied electrical pulse, causes an instantaneous change in the pressure distribution within the tube. This pressure distribution acts, in turn, as the initial condition for the acoustic wave propagation.

We recall the one-dimensional wave equation of linear acoustics in terms of pressure $p(x, t)$ or displacement $\zeta(x, t)$.

$$c^2 p_{xx} = p_{tt} \quad \text{or} \quad c^2 \zeta_{xx} = \zeta_{tt}, \tag{1}$$

where subscripted variables denote partial derivatives and c represents the sound speed in the fluid. The relationships between p and ζ, as well as particle velocity u and ζ, are

$$p = -\rho_0 c^2 \zeta_x, \qquad u = \zeta_t, \tag{2}$$

where ρ_0 is the fluid density.

The general solution of the pressure wave equation in Eq. (1) is

$$p(x, t) = f(x - ct) + g(x + ct), \tag{3}$$

which represents the sum of two pressure profiles: a profile f that propagates in the positive x-direction (to the right) and a profile g that propagates in the negative x-direction (to the left) at speed c. This general solution can be used to derive the d'Alembert solution of an initial value problem for waves in a tube of infinite length as

$$p(x, t) = \frac{1}{2}[\phi(x - ct) + \phi(x + ct)] + \frac{1}{2c}\int_{x-ct}^{x+ct} \theta(s)ds, \tag{4}$$

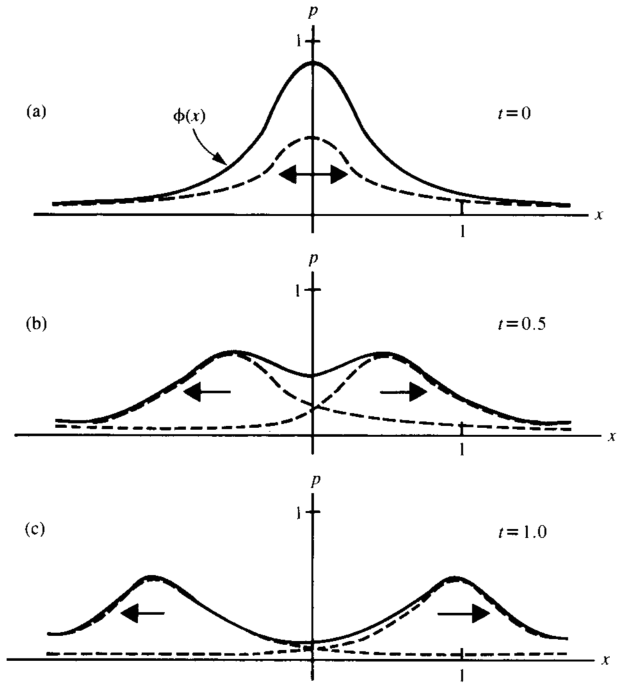

Figure 8 Division and propagation of initial pressure distribution $\phi(x)$ in an infinitely long tube.

where the functions ϕ and θ describe the initial conditions

$$p(x, 0) = f(x) + g(x) = \phi(x),$$

$$p_t(x, 0) = -cf'(x) + cg'(x) = \theta(x). \tag{5}$$

Consider the case of an infinite tube in which the initial pressure distribution $\phi(x)$ is shown in **Figure 8(a),** and for which the initial rate of pressure $\theta(x)$ vanishes. Equation (4) gives the pressure at subsequent times as

$$p(x, t) = \frac{1}{2}\,[\phi(x - ct) + \phi(x + ct)], \tag{6}$$

and **Figures 8(b)** and **8(c)** show the pressure distributions at times $t = 0.5$ and 1.0. In accordance with Eq. (6), the initial pressure, at $t = 0$, splits itself into halves that propagate in opposite directions at speed c. The pressure at subsequent times is merely the sum of the two displaced halves.

When an obstruction occurs at some location in the tube, part of the pressure wave is transmitted and part of it is reflected. The transmission and reflection coefficients associated with the obstruction determine the amplitudes and phases of the transmitted and reflected waves. The simplest cases to analyze are the idealized open and closed ends. These are also appropriate first approximations to the end conditions in the drop-on-demand "squeeze" tube assembly used here (Fig. 1). The end with the nozzle plate attached can be considered as approximately closed, since the nozzle opening is a small

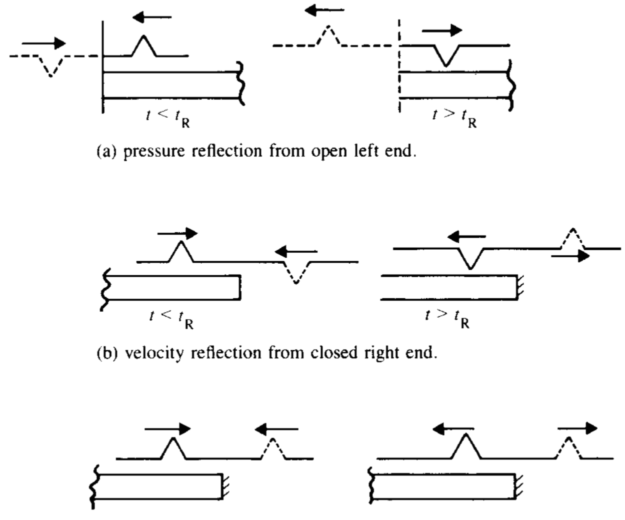

(a) pressure reflection from open left end.

(b) velocity reflection from closed right end.

(c) pressure reflection from closed right end.

Figure 9 Pressure and velocity reflections from open and closed ends of a tube. Reflection is assumed to occur at a time t_R.

fraction of the tube cross-sectional area. The supply end can be considered as approximately open, since the inside diameter of the supply tube is considerably larger than the inside diameter of the squeeze tube. These simple approximations should be good enough to determine whether the analysis used here is applicable. Refinements in the resulting reflection coefficients can then be made if necessary.

The pressure reflections from open and closed ends are obtained from the boundary conditions with the use of Eqs. (1) and (2). Consider first the open end in **Figure 9(a),** where the boundary condition is assumed to be zero pressure. This boundary condition is satisfied by superimposing on the incident pressure wave a similar pressure wave of opposite sign outside the tube that is traveling in the opposite direction at the same distance from the end as the incident wave. Consider next the closed end in **Figure 9(b),** where the boundary condition is zero velocity. Since the displacement $\zeta(x, t)$ satisfies the same wave equation as the pressure [Eq. (1)], and since the velocity $u(x, t)$ is related to $\zeta(x, t)$ by the second part of Eq. (2), it follows that the velocity also satisfies a similar equation. Therefore displacement and velocity have propagating wave solutions similar to the one given in Eqs. (3)–(6) for pressure. If

$$\zeta(x, t) = f(x - ct), \tag{7}$$

then

$$u = -cf', \qquad p = -\rho c^2 f', \tag{8}$$

whereas if

$$\zeta(x, t) = g(x + ct), \tag{9}$$

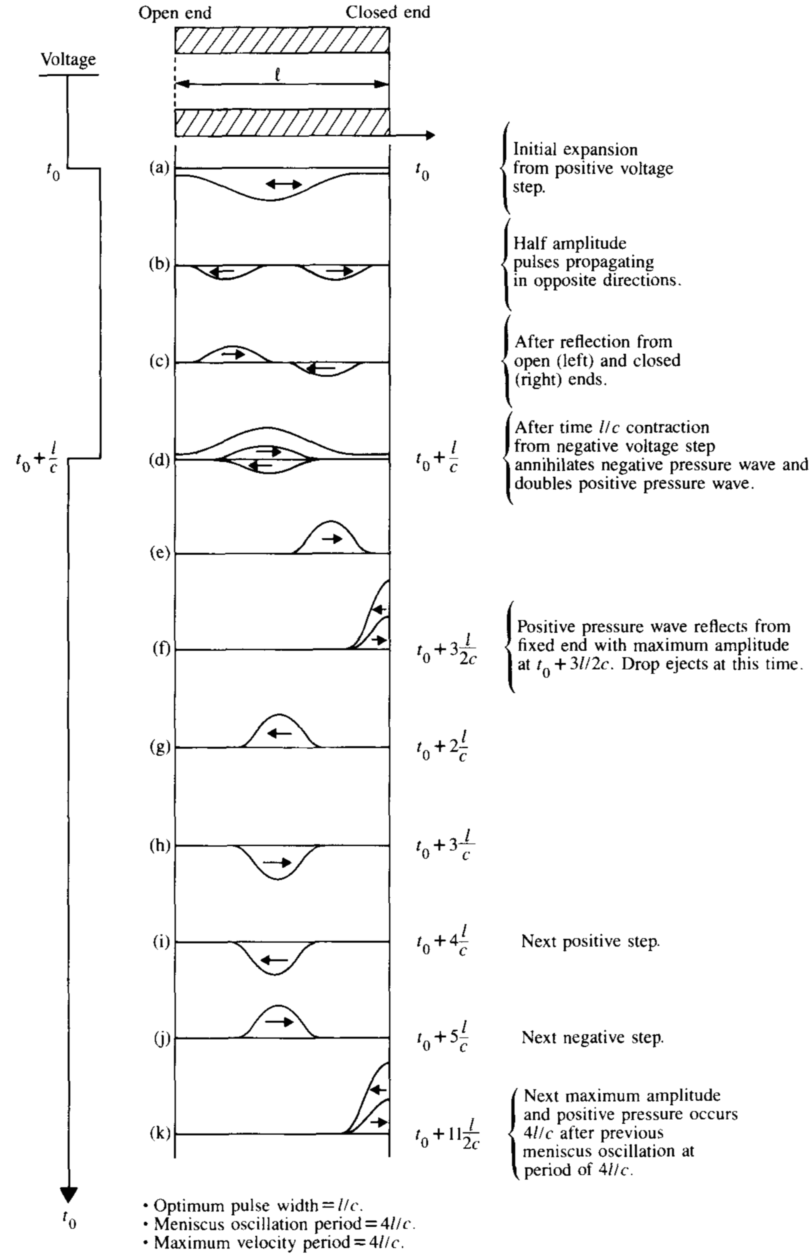

Figure 10 Propagation and reflections of initial pressure pulse in an open-closed squeeze tube.

then

$$u = cg', \qquad p = -\rho c^2 g'. \tag{10}$$

Therefore, we see that velocity and pressure have the same sign for waves propagating in the positive x-direction, but they have opposite signs for waves propagating in the negative x-direction. Figure 9(b) shows a velocity pulse reflection from a closed end, and **Figure 9(c)** shows the associated pressure pulse reflection from the same closed end. Thus a pressure wave changes sign as it reflects from an open end and it retains its sign as it reflects from a closed end.

We now consider an initial value problem in a finite-length open-closed tube of length l, and attempt to explain the experimental observations presented in the first part of this paper. We assume that the voltage applied to the PZT tube is a positive rectangular function. It has been determined (see [4]) that for the polarization and polarity in the configurations used in this study, a positive voltage step causes the inner radius of the tube to increase. Likewise, a negative voltage step causes a decrease in its inner radius. The response of the tube can be assumed to follow the voltage pulse with very little oscillation or ringing (see [4]).

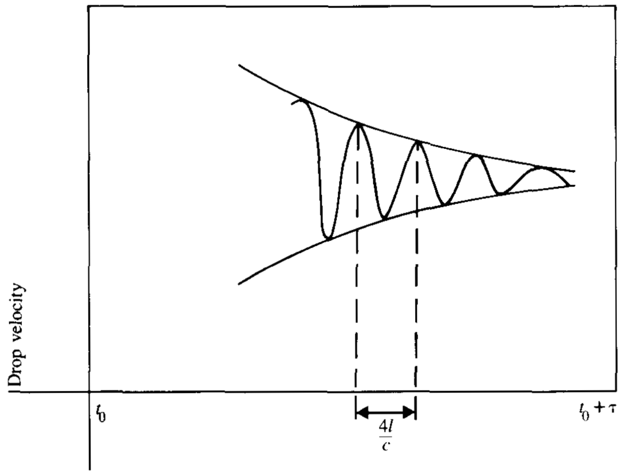

Figure 11 Predicted dependence of drop velocity on period in a periodic application of voltage pulses.

Figure 10 shows a sequence of expected pressure pulse propagations and reflections. In Fig. 10(a) is shown the assumed initial negative pressure distribution resulting from the sudden expansion of the squeeze tube caused by the positive voltage step at the initial time t_0. This initial pressure profile is assumed to some extent for convenience of analysis, but it should also be a reasonably good approximation of what actually occurs. It must be negative everywhere; it must decrease in amplitude to zero toward the open end, and should decrease slightly in amplitude toward the nozzle end since the meniscus can flex to release the partial vacuum at that end. Figure 10(b) shows the initial pressure profile split into its halves, which should propagate in opposite directions according to Eq. (6). Figure 10(c) shows the expected two propagating pressure waves after one reflection from the open (left) and closed (right) ends, according to the reflection rules established in this analysis. Figure 10(d) shows the two pressure waves after each has traveled a distance l. At the instant $t_0 + l/c$, the two waves should add to give zero total pressure, but this should not interrupt their propagation. If at this instant the voltage steps down to zero, the tube should contract and thereby add a new initial pressure distribution which is identical, except for its sign, to the original initial pressure distribution at t_0 [Fig. 10(a)]. The result is that the left propagating negative pressure wave should be annihilated and the right propagating positive pressure wave doubled. The pressure wave expected shortly afterwards is shown in Fig. 10(e). By applying the voltage down-step at exactly $t_0 + l/c$, the amplitude of the pressure wave should thus have been optimally enhanced.

Figure 10(f) shows the expected double-amplitude pressure wave midway in its reflection from the nozzle. One half of the wave continues to the right and the other half continues to the left. At this instant, $t_0 + 3l/2c$, the pressure at the nozzle should be four times the original pressure wave amplitude. This is expected to be the condition most favorable for drop ejection. Therefore, our analysis indicates that the optimal pulse width is the time period l/c, and that drop ejection should begin to occur after a delay of $3l/2c$ after the initial voltage step.

In the absence of damping, if no other voltage step is applied, the later sequence of pressure waves should occur as shown in Parts (g–k) of Fig. 10. We observe that the next large positive pressure wave should arrive at the nozzle at the instant $t_0 + 11l/2c$, which is $4l/c$ after the drop ejection. Thus the meniscus oscillation period predicted by this model would be $4l/c$.

If the reflection coefficients at the ends are less than unity in amplitude and viscous effects diminish the amplitude of the pressure wave as it propagates, the amplitude of the meniscus oscillations that occur after drop ejection would be expected to decrease with time. In order to eject subsequent drops with the smallest voltage step, advantage must be taken of the residual pressure wave that is reflecting back and forth between the ends of the tube. From our experimental results, the drop-formation time is typically greater than $4l/c$ and therefore more than one large pressure wave arrives at the nozzle before the drop separates. Thus, if the voltage step for the next drop is applied too soon, the second drop is ejected prior to separation of the first drop and two drops may be still connected after ejection. Nevertheless, an opportunity presents itself periodically at time intervals of $4l/c$ for taking advantage of the residual pressure wave. In order to synchronize with one of the positive pressure waves, the positive voltage step must be applied at a time $3l/2c$ prior to the arrival of this wave at the nozzle. At an instant $2l/c$ after the arrival of a pressure wave, a rarefaction (negative pressure) wave arrives. It would be least favorable to synchronize the positive voltage step at the instant $3l/2c$ prior to the arrival of this negative pressure pulse at the nozzle.

On the basis of this discussion, it is expected that a plot of drop velocity as a function of period, in a periodic application of the voltage step, would have maxima separated by $4l/c$, as indicated in **Figure 11.** Because of viscous and reflection losses the enhancement effect of the residual pressure wave should diminish with time.

Summary and conclusions

The experimental observations show that the operation of drop-on-demand ink jet nozzle assemblies comprised of piezoelectric transducer tubes with a silicon plate nozzle attached to one end and an ink supply connected to the other end depends strongly on the length of the cavity. Four measurable quantities appear to be linearly dependent on this length and on the speed of sound in the ink: the optimum (rectangular) pulse width is equal to l/c; the delay time before the meniscus starts to protrude is equal to $3l/2c$; the period of meniscus oscillation is equal to $4l/c$; and the period of low-frequency resonant and antiresonant synchronous operation is equal to $4l/c$. There are some deviations from these linear dependencies, as shown in Fig. 3, but the preponderance of data support this linear behavior with length.

The linear behavior follows from a simple one-dimensional acoustics analysis with reflection coefficients based on the presence of a closed end at the nozzle and an open end at the supply. Expansions and contractions of the tube resulting from an applied voltage pulse generate rarefaction and compression waves, which, after appropriate end reflections, reinforce or interfere with each other to enhance or impede the velocity of the ejected drops. An upper limit on the frequency of this resonance type phenomenon is set by the time required for the separation of a drop. Several reflected waves can contribute to the process. In the higher frequency range, resonances and antiresonances in the operation occur in accordance with the fundamental and higher harmonics.

Acknowledgment
We appreciate the assistance of Robert Payne in the experimental part of this study.

References
1. J. D. Beasley, "Model for Fluid Ejection and Refill of an Impulse Drive Jet," *J. Appl. Photogr. Eng.* **3**, 78–82 (1977).
2. E. L. Kyser, L. F. Collins, and N. Herbert, "Design of an Impulse Ink Jet," *J. Appl. Photogr. Eng.* **7**, 73–79 (1981).
3. H. Gerhauser, K. H. Hirschmann, F. C. Lee, and F. E. Talke, "The Effect of Pulse Shape on the Drop Volume and the Frequency Response of Drop-on-Demand Ink Jet Transducers," *SID-83 Digest* **14**, 110–111, (1983).
4. N. Bugdayci, D. B. Bogy, and F. E. Talke, "Axisymmetric Motion of Radially Polarized Piezoelectric Cylinders Used in Ink Jet Printing," *IBM J. Res. Develop.* **27**, 171–180 (1983).

Received October 18, 1983; revised December 30, 1983

David B. Bogy *Department of Mechanical Engineering, University of California, Berkeley, California 94720.* Dr. Bogy is a Professor of Applied Mechanics at Berkeley and since 1972 has been a consultant to the applied technology group at the IBM Research laboratory in San Jose. His current technical interests include work in elastic wave scattering and mechanics of magnetic recording and printing technology. He received a B.A. in geology and mechanical engineering and an M.S. in mechanical engineering in 1959 and 1961, both from Rice University, Houston, Texas, and a Ph.D. in applied mathematics in 1966 from Brown University, Providence, Rhode Island. After postdoctoral work in elasticity at the California Institute of Technology, he joined the faculty of the University of California at Berkeley in 1967. Dr. Bogy is a member of the American Society of Mechanical Engineers and Sigma Xi.

Frank E. Talke *IBM Research Division, 5600 Cottle Road, San Joser, California 95193.* Dr. Talke joined IBM in 1969 at the San Jose Research laboratory and is currently on sabbatical leave as a visiting professor at the University of California at Berkeley. Previously he was manager of the device mechanics group in the applied science complex in San Jose, where he initiated the work on drop-on-demand ink jet technology. Prior to that, he studied the mechanical aspects of magnetic recording technology. He attended the University of Stuttgart, Germany, where he received a Diplom-Ingenieur degree (M.S.) in mechanical engineering in 1965, and the University of California at Berkeley, where he received a Ph.D. in mechanical engineering in 1968.